RESEARCH ARTICLE

Title: A Memristive Element based on Electrically Controlled Single-Molecule Reaction

Haipeng B. Li†, Behabitu E. Tebikachew‡, Cedrik Wiberg‡, Kasper Moth-Poulsen*‡, Joshua Hihath*†

† Department of Electrical and Computer Engineering, University of California Davis, Davis, California 95616, United States
‡ Department of Chemistry and Chemical Engineering, Chalmers University of Technology, 41296 Gothenburg, Sweden

Abstract: The exponential proliferation of data during the Information Age has required the continuous exploration of novel storage paradigms, materials, and devices with increasing data density.[1] As a step toward the ultimate limits in data density, the development of an electrically-controllable, single-moleculememristive element is reported. In this device, digital information is encoded through switching between two isomer states by applying a voltage signal to the molecular junction, and the information is read-out by monitoring the electrical conductance of each isomer. The two states are cycled using an electrically-controllable local heating mechanism for the forward reaction[2–4] and catalyzed by a single charge transfer process for the reverse switching.[5–7] This single-molecule device can be modulated *in situ*, is fully reversible, and does not display stochastic switching. The I-V curves of this single molecule system also exhibits memristive character. These features suggest a new approach for the development of molecular switching systems and storage class memories.

Introduction

The increases in speed, scalability, and accessibility of computational technologies has resulted in a nearly insatiable desire for advanced data storage technologies. Conventional technologies such as hard-disk drives and FLASH memories are facing fundamental physical challenges as the feature sizes enter the quantum regime. Confronting these obstacles has led to the emergence of a variety of novel technological platforms that aim to extend the exponential improvement of electronic elements “beyond silicon”.[8] Molecular-scale electronics has been at the forefront of this approach,[9,10] aiming to develop new instantiations of wires,[11,12] diodes,[13,14] transistors,[15] and photoswitches[16] that operate at the single-molecule level. Here, we introduce the development of a single-molecule memristive element in which information is encoded by electrically controlling the isomerization processes in a molecule that is traditionally activated photochemically (**Figure 1b**). The electrically induced isomerization processes within a molecular junction are particularly different from reactions in free molecules which would lead to new insight in understanding chemical reaction in a single molecule level.

Results and Discussion

The memristive element consists of a bicyclic norbornadiene (NB) derivative with oligophenylene-ethylene (OPE) side groups that are terminated with thiol linkers that allow attachment to two gold electrodes in a single-molecule break junction (SMBJ) system (**Figure 1a**).[17] This NB-state configuration provides a conductive, conjugated pathway from one gold electrode to the other through the molecular backbone, and therefore exhibits a higher conductance, see **Figure S1.**[18] In conventional photochemical measurements, the molecule is photo-isomerized with UV light and the NB-state molecule is switched to the quadricyclane (QC) form, which breaks the conjugation pathway and results in a lower conductance value.[18] Once in the QC-state, the system eventually thermally relaxes back to the NB-state. The photochemically induced NB-QC-NB transition pathway is a well-studied process which has recently gained attention as a possible methodology for thermal storage of solar energy.[19–23] However, we find that the reaction mechanisms are significantly different when the system is placed in a single-molecule junction and electrically stimulated. As shown here, the forward NB-QC process is thermally activated by electrically heating the junction, and the reverse process requires a high bias and a single electron transfer (SET) between the molecule and the gold contacts to induce the back-isomerization process (**Figure 1c**, blue and orange, respectively). These two reactions are reversibly controlled *in situ* by modulating the bias between the two switching potentials (**Figure 1b**).

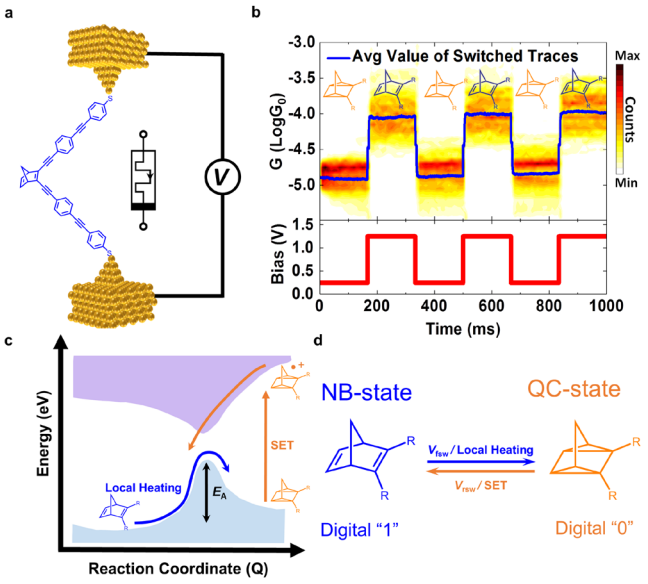

Figure 1. a) Schematic of the molecular device with a modulating bias. b) Reversible switching behavior of single-molecule devices and the applied waveform. 17.5% (126 out of 719) devices completed all 3 cycles. c) Energy landscape of isomerization processes. Blue arrow and orange arrows indicate the electrically-controlled forward and reverse switching processes respectively. d) Schematic describing the processes for controlling the NB-QC switching within a molecular junction (blue and orange arrow). The switching processes within a molecular junction are controlled in the forward direction (NB to QC) by electrically controlling the local temperature and in the reverse process (QC to

NB) by catalyzing the reaction through a single electron transfer (SET) process. These two states possess different conductance values and can be used to encode digital information.

We start by investigating switching from the NB-state to the QC-state as shown in **Figure 2**. The SMBJ experiment (see Experimental Section) is performed by repeatedly making contact between two electrodes and measuring the conductance as they are separated. Statistical analysis of the resulting conductance vs. distance traces results in histograms (**Figure 2a** and **Figure 2b**) which reveal the most probable conductance value of a single-molecule device. When starting with molecules in the NB-state in vacuum (~1 × 10^{-6} Torr), at room temperature, and at low biases (< 50 mV), only a single-peak appears in the conductance histogram, which corresponds to the conductance of a single NB-molecular junction (1.2 × 10^{-4} G_0).[18] However, as the bias is increased, a second peak begins to appear at 1.9 × 10^{-5} G_0 which corresponds to the QC-state, the number of counts at this value increases as the bias increases. Then, once the bias reaches 150 mV, the NB peak can no longer be discerned (**Figure 2a**). To provide a quantitative description of the switching, we define the NB to QC "forward switching potential" (V_{fsw}) as the point where an NB-state and a QC-state have equivalent probability of appearing in a SMBJ experiment dataset (**Figure S2**). At room temperature, under vacuum, V_{fsw} = 101 ± 3 mV (shown by red arrow in **Fig. 2a**). However, the results are markedly different at a T_0 of 78 K (**Fig. 2b**). Here, we do not begin to see significant changes in the population until we are near 150 mV, and the system is not dominated by the QC state until we reach a value of 250 mV. In this case the value of V_{fsw} is much higher, 183 ± 4 mV. Notably, in both of these cases, the forward switching potential is much smaller than the energy of the absorbed photon in photochemical experiments (~3 eV),[18] suggesting a significantly different reaction pathway.

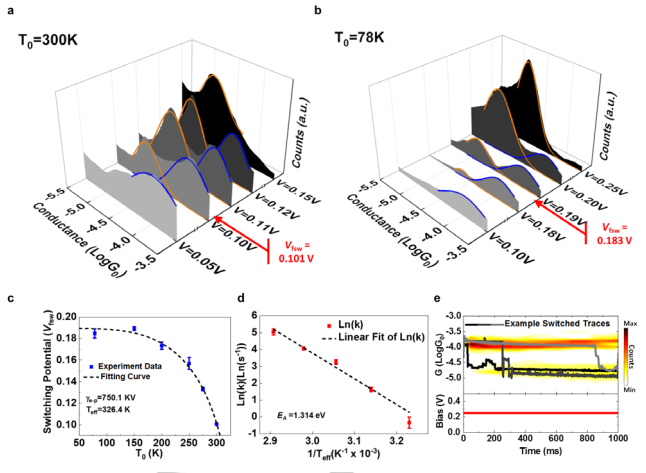

Figure 2. Electrical Control of the NB to QC reaction pathway. a) Conductance histograms displaying switching behavior at room temperature in vacuum. At low biases, only the NB-state is observed (fitted with blue curves), and at higher biases only the QC-state is observed (fitted with orange curves). At V_{fsw} = 101 ± 3 mV the two states have an equal probability. b) At 78K V_{fsw} = 183 ± 4 mV. c) V_{fsw} as a function of environmental temperature demonstrating local heating behavior. d) By examining the transition rate for this system, we extract an activation barrier E_A = 1.314 eV for the NB to QC transition. Error bars in c) and d) are the standard deviations from 3 experiments. e) 2D histogram showing the change in conductance as a function of time when a 0.25 V bias is applied to the junction. 44.5% (181 out of 407) of the junctions undergo a NB to QC transition.

While a variety of stimuli (electrical field, vibrionic mode, local temperature, etc.) can induce isomerization processes,[24–26] the change in V_{fsw} as a function of T_0 suggests the switching behavior originates from a thermally activated process due to electronic local heating of a molecular junction.[4,27,28] Moreover, a control experiment with various bias voltages in a solution phase (mesitylene) has been performed.(SI, Sec. 3) and no obvious peak population shift is observed up to 1000 mV (**Figure S4**). Previous studies have shown that rapid phonon relaxation (< 10 ps) from various molecules to the solvent environment can lead to a fast cooling effect[29–32] and a molecular junction with surrounding environment would have a lower local temperature compared with an isolated molecular junction.[33] Therefore, the absence of a population shift in solvent further reinforces the notion that forward switching process is thermally driven.

To quantitatively explore the local heating mechanism in detail we repeated the SMBJ experiments across temperatures ranging from 300 K to 78 K and found that V_{fsw} changed from 101 ± 3 mV to 183 ± 4 mV over this range. To extract the local temperature of the junction as a function of the environment temperature and applied bias, we utilize a model developed by Di Ventra et al.[2–4].

$$T_{\mathrm{eff}}^4 = T_0^4 + \gamma_{\mathrm{e-p}}^4 V_{\mathrm{b}}^2. \qquad (1)$$

where T_0 is the environment temperature and $\gamma_{\mathrm{e-p}}$ is a generalized electron-phonon coupling coefficient defined by the molecular junction structure. The effective temperature (T_{eff}) depends on the coupling between tunneling current with the phonon modes of molecular junction as well as the elastic phonon scattering (heat dissipation into electrodes) between gold contact lattice and the molecule. Assuming that the effective temperature of the molecular junction (T_{eff}) is the same at each switching potential and fitting yields $\gamma_{\mathrm{e-p}} = 750.1\ \mathrm{KV}^{-1/2}$ and $T_{\mathrm{eff}} = 326.4$ K (**Figure 2c**, black dashed line). The agreement of experimental data and the fitting curves in **Figure 2c** supports the thermally-driven NB to QC isomerization process. The extracted electron-phonon coupling coefficient $\gamma_{\mathrm{e-p}} = 750.1\ \mathrm{KV}^{-1/2}$ for NB state, and is consistent with the trend from other experiment work[4,27] which suggest that π-bonding throughout a molecular system yields larger electron-phonon couplings. We also extracted the activation barrier for the switching process by treating the isomerization process as a thermally-activated first order reaction with $k_{fsw} = A \cdot exp(-E_A/k_B T_{eff})$, where E_A is the activation barrier, k_B is the Boltzmann constant, and k_{fsw} is the transition rate from NB to QC. Here, k_{fsw} is estimated from the probabilities of the two states through sorting the state of the single traces in the 1D conductance histograms (Eqn. S1) at bias ranging from 170 mV to 210 mV with T_0 = 78 K. Since the QC state should have a smaller $\gamma_{\mathrm{e-p}}$ due to the saturated bond at the center, a much smaller effective temperature is expected. Therefore, the spontaneous relaxation from QC to NB is assumed to be negligible in this case. T_{eff} is then determined using Eq (1) and the fitted value of $\gamma_{\mathrm{e-p}}$. From this information, we were able to plot the transition rate as a function of $1/T_{\mathrm{eff}}$ (**Figure 2d**, SI Sec.4), and found an activation barrier of E_A = 1.314 eV. In solution phase, this potential barrier is estimated to be in the range of 1.5 ~ 2.0 eV.[18,19] These results indicate that a thermally activated pathway is possible, though there are changes in the energy landscape

when the molecule is bound in the junction vs. the solution pathway.[34].

Finally, we examined the switching process *in situ* by holding a molecular junction and stepping the bias to 250 mV for 1000 ms (**Figure 2e**) under T_0=78 K. In this case, the NB to QC transition occurred probabilistically with 44.5% of the junctions switching within the hold time. Interestingly, stochastic switching between the states rarely occurred. Both of these observations are consistent with a thermally-induced switching mechanism as i) small variations in configuration will affect the power dissipation and heating of the junction thus modifying the switching time, and ii) the QC-state is expected to have a smaller γ_{e-p} which implies the junction will cool-down after switching into the QC-state especially at a low T_0 and allow the QC molecule to stabilize in this configuration without changing the bias.

Having developed an understanding of the switching process from the NB-state to the QC-state, we now examine the reverse process. At much higher biases (0.75 V to 1.5 V) we once again began to observe differences in the populations of NB-state and QC-state in the conductance histograms (**Figure 3a,b**), and we are again able to estimate a potential at which the two populations have equal probability in a SMBJ, which we term as the "reverse switching potential" (V_{rsw}). For this reaction there was no obvious change in V_{rsw} (defined similarly as V_{fsw}, SI Sec. 2) ranging from 78 K to 300 K (**Figure 3c**), which indicates that local heating is not the dominant mechanism in the QC to NB transition.

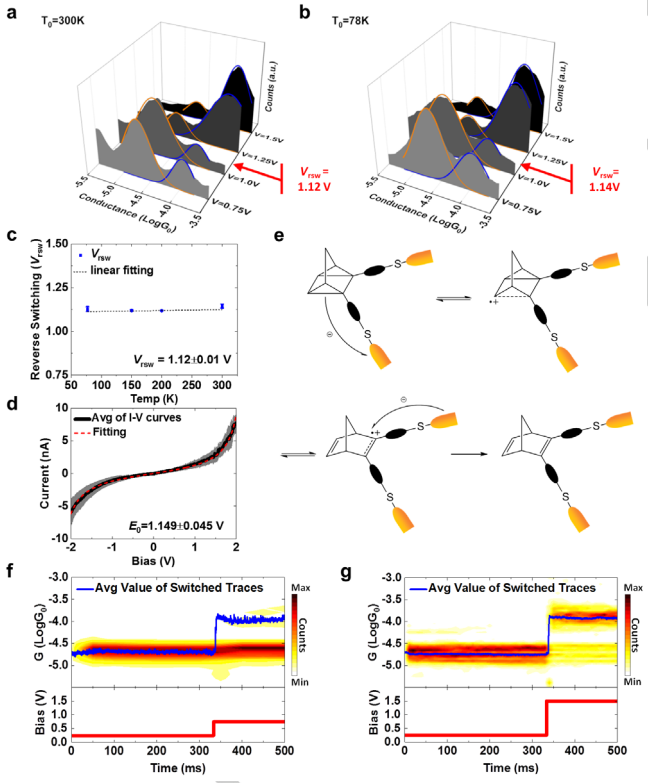

Figure 3. Electrical Control of the QC to NB reaction pathway. a) Conductance histograms showing the high-bias switching behavior of the QC system at room temperature. At 0.75V most molecules are in the QC-state. By 1.5 V the system is again dominated by the NB-state. b) Conductance histograms obtained at 78K showing similar behavior. c) Temperature independence of the reverse switching potential (V_{rsw}). Error bars are the standard deviations from three experiments. d) Average *I-V* characteristics fit with a single-level model demonstrating that the energy offset between the molecular orbital and the Fermi energy of the electrodes is similar to the reverse switching potential. Grey area corresponds to standard deviation of 24 *I-V* curves e) Schematic illustration of SET assisted QC to NB mechanism when applied bias is higher than the reverse switching voltage. Single-sided arrow indicates the electron transfer through the molecular orbital not through the space f) 2D conductance histogram displaying the switching from QC to NB when a 0.75V step function is applied, 4.8% (5 out of 104) curves switch. g) Similar histogram displaying behavior when 1.5V is applied. 70.6% (60 out of 85) junctions switch in this case.

Previous studies have shown that the QC to NB isomerization process can be catalyzed by a Single Electron Transfer (SET) reaction, where radical formation to QC$^{\bullet+}$ is followed by isomerization to NB$^{\bullet+}$, and then reduction back to the neutral NB-state (see SI Sec. 9 for cyclic voltammetry experiments).[23,35–37] The energy barrier for this process is smaller than that for the direct QC to NB transition.[23,35–37] Moreover, in a molecular junction oxidation can easily occur when the Fermi level of the electrode is aligned with the HOMO level of the molecule.[38,39] To explore this possibility, we examined the current-voltage (*I-V*) characteristics of single-molecule junctions in the QC-state that did not show switching behavior, and adopted the Breit-Wigner single-level formula[40,41] to estimate the energy difference (E_0) between the HOMO-level of molecule in the QC-state and the Fermi energy of the gold electrode (Eqn S2). Using this model to fit 24 *I-V* curves measured on QC-state molecular junctions yields an energy difference of E_0 = 1.149 ± 0.04 eV (**Figure 3d**), and a coupling coefficient Γ of 6.69 ± 0.03 meV. These values coupled with the propensity of this molecular system for SET-catalyzed relaxation in the QC suggests that the high bias applied to the junction could induce the SET-catalyzed reaction process. As described in **Figure 3e**, when the applied bias is large enough for the electrode to oxidize the QC state molecule, a single electron could transfer (indicated by single-sided arrow) to the electrode through the molecular orbital through the phenyl rings and become QC$^{\bullet+}$. A QC radical cation would relax to an NB radical cation rapidly due to the decreased energy barrier and gain an electron from electrode to become a neutral state. Similar SET-catalyzed reaction process is demonstrated in metal catalyzed reactions[35,36] as well as electrochemical process,[23,37] and these results are also consistent with recent reports describing stabilization of charged transition states in molecular junctions.[42] To further test this hypothesis, *in situ* QC to NB switching experiments are performed using the bias waveform shown in Figure 3f-g. First, a long bias window (330 ms) at 250mV is applied to ensure the junctions are in the QC-state, then a step function is applied to switch the system to the NB-state. In this case, no delay was observed in the switching. Either the junction switched immediately, or did not switch at all, again confirming a different switching mechanism from the NB to QC process. In the case where the bias is stepped to 0.75 V, 4.8% of the junctions switch to the NB-state. Alternatively, stepping to 1.5 V results in 70.6% of the junctions switching (**Figure 3f,g**).

It is generally true that local heating effect still exist in the reverse QC to NB SET assisted switching process. But since no temperature dependence is observed in the reverse process, local heating is not playing the dominant role. This is likely due to a couple of reasons. First, because the QC-state molecule is not conjugated throughout the molecular backbone and the conductance is lower, it is expected that the electron-phonon

coupling is smaller. Additionally, at high biases, it has been shown that electron-electron coupling must be taken into account which causes the junction to cool.[4,27,43] The combination of heating effects in the two states and the accessibility of SET processes in the QC-state thus combine to create a system that can be switched bidirectionally and non-stochastically using only the bias as the control barrier. These factors thus open up the possibility of utilizing the system in a memory configuration where different biases are used to set the molecule into different states.

To explore the utility of this molecular system as a memory element, we applied a specific bias waveform to the molecular junction after it has been formed, to examine the memory behavior for each case. There are three steps to the applied waveform (**Figure 4a, b**) corresponding to "Detect", "Write" and "Read" in a memory device. Figure 4a depicts writing from QC to NB and testing the NB volatility. The three bias steps are i) 0.25 V to detect the QC-state, ii) 0.75 V to write the NB-state, and iii) 0.1 V to read the NB-state with a potential low enough to not cause switching effects. Here, 64.3% of the curves that switch to the NB-state remain there after the bias is reduced in step iii). Figure 4b illustrates the memory behavior when switching from NB-state to QC-state. Here the waveform voltages are i) 1.25 V, ii) 0.25 V, and iii) 0.1 V corresponding to the "Detect", "Write", and "Read" steps in the process. In this case, after a molecule is switched to the QC-state, 95.8% of curves remain there during the "Read" cycle. Furthermore, a three cycle square wave is applied to the molecular junction as shown in **Figure 1b** with a high bias 1.25 V and a low bias 0.25 V. Around 17.5 % of the traces respond to the applied signal instantaneously. The rest of the curves which partially respond to the signal could be found in SI **Figure S8**. **Figure 4c** demonstrates the study on I-V characteristics of the NB-QC molecular junction. A molecular junction in the QC-state is formed at the beginning of the I-V sweep (by applying a bias of 0.25V when picking up the molecule). A 0 V – 1.5 V – 0 V bias voltage is then applied to the QC junction with a sweep time of 0.1 sec. 159 out of 296 total curves demonstrate switching behavior during the I-V sweep and the I-V traces are overlaid to build the 2D histogram shown in **Figure 4c**. Blue arrows are guides to the eyes. Example curves of the I-V traces are presented in SI **Figure S10**. The ideal I-V hysteresis (**Figure S10a**) demonstrates NB to QC switching at around 1.5 V and the trace remains at NB-state. In other cases (**Figure S10b**), we observe the competing process between the forward switching and reverse switching in the mid-range bias which is consistent with our expectation. The hysteresis I-V characteristics would lead to application of memristive device. Details of the I-V characteristics could be found in the SI Sec. 10.

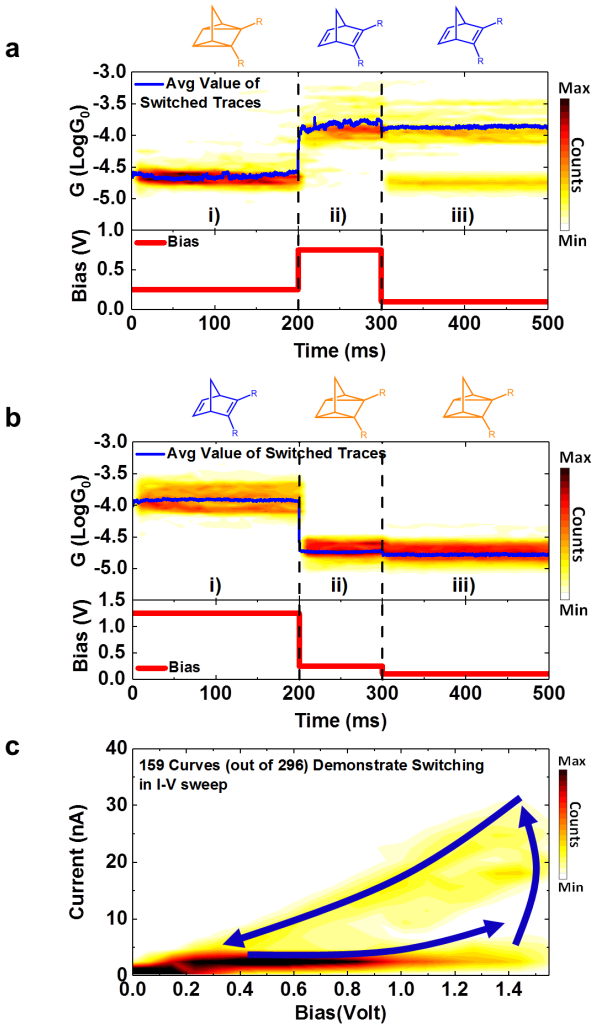

Figure 4. a) 2D conductance histogram showing behavior when a three-step waveform is applied to first "Detect" the QC-state (200 ms) then "Write" the NB-state (0.75 V, 100 ms), and finally to "Read" the NB-state (0.1 V, 200 ms). When the large bias is removed most of the curves (64.3%, 27 out of 42) can remain in the high conductance state, allowing the system to operate as a memristive element. b) 2D conductance histogram showing conversion to the QC-state with high reliability and low volatility. (95.8%, 92 out of 96 remain at QC). c) Memristive behavior of NB-QC system in I-V sweep. Blue arrows are guides to the eye. The 2D histograms contains 159 curves (out of 296) showing switching hysteresis behavior in the I-V sweep. Sweeping bias is from 0 V to 1.5 V and back to 0 V in 0.1 sec.

Conclusion

In conclusion, we have demonstrated that the photoactive norbornadiene molecular switch can be isomerized electrically *in situ* to realize an electrically-controllable single-molecule memristive element. The switching mechanisms are significantly different from those observed in photochemical measurements on the same system. The NB to QC transition arises from a local heating effect due to current flow and a SET reaction facilitates the QC to NB reaction process. This work suggests unique avenues for modulating isomerization processes in single-

molecule devices and demonstrates that photoactive molecular devices may operate as electrically-controllable single-molecule memristive element elements. With continued work, the intrinsic character of the molecule could also be improved by continued engineering of the molecule structure. Both the energy barrier between the two states as well as the electron-phonon coupling coefficient could be tuned and a single molecule device with better nonvolatility could be achieved, and further progress toward developing molecular memristive devices could be made.

Acknowledgements

The authors would like to dedicate this work to the memory of Dr. Nongjian Tao, an incredible, mentor, friend, colleague and scientist. The authors also acknowledge financial support from the ONR (N000141612658) (JH), the NSF/SRC (1807555), and the European research council ERC-StG SIMONE grant number 337221 (BET, KMP).

Keywords: molecular electronics • single molecule switch • molecular memristive element • memristor

[1] M. Winans, D. Faupel, A. Armstrong, J. Henderson, E. Valentine, L. McDonald, D. Walters, J. Waite, M. Trapani, E. Magill, *10 Key Marketing Trends for 2017 Customer Expectations and Ideas for Exceeding Customer Expectations*, **2016**.

[2] Y. C. Chen, M. Zwolak, M. Di Ventra, *Nano Lett.* **2003**, *3*, 1691–1694.

[3] R. D'Agosta, N. Sai, M. Di Ventra, *Nano Lett.* **2006**, *6*, 2935–2938.

[4] Z. Huang, F. Chen, R. D'Agosta, P. A. Bennett, M. Di Ventra, N. Tao, *Nat. Nanotechnol.* **2007**, *2*, 698–703.

[5] N. Borsub, C. Kutal, *J. Am. Chem. Soc.* **1984**, *106*, 4826–4828.

[6] H. Ikezawa, C. Kutal, *J. Org. Chem.* **1987**, *52*, 3299–3303.

[7] G. W. Sluggett, N. J. Turro, H. D. Roth, *J. Phys. Chem. A* **1997**, *101*, 8834–8838.

[8] N. Mathur, *Nature* **2002**, *419*, 573–575.

[9] T. A. Su, M. Neupane, M. L. Steigerwald, L. Venkataraman, C. Nuckolls, *Nat. Rev. Mater.* **2016**, *1*, 1–15.

[10] D. Xiang, X. Wang, C. Jia, T. Lee, X. Guo, *Chem. Rev.* **2016**, *116*, 4318–4440.

[11] L. A. Bumm, J. J. Arnold, M. T. Cygan, T. D. Dunbar, T. P. Burgin, L. Jones, D. L. Allara, J. M. Tour, P. S. Weiss, *Science (80-.).* **1996**, *271*, 1705–1707.

[12] M. H. Garner, H. H. Li, Y. Chen, T. A. Su, Z. Shangguan, D. W. Paley, T. Liu, F. Ng, H. H. Li, S. Xiao, et al., *Nature* **2018**, *558*, 416–419.

[13] A. Aviram, M. A. Ratner, *Chem. Phys. Lett.* **1974**, *29*, 277–283.

[14] I. Díez-Pérez, J. Hihath, Y. Lee, L. Yu, L. Adamska, M. A. Kozhushner, I. I. Oleynik, N. Tao, *Nat. Chem.* **2009**, *1*, 635–41.

[15] S. J. Tans, A. R. M. Verschueren, C. Dekker, *Nature* **1998**, *393*, 49–52.

[16] C. Jia, A. Migliore, N. Xin, S. Huang, J. Wang, Q. Yang, S. Wang, H. Chen, D. Wang, B. Feng, et al., *Science (80-.).* **2016**, *352*, 1443–1445.

[17] B. Xu, N. J. Tao, *Science (80-.).* **2003**, *301*, 1221–1223.

[18] B. E. Tebikachew, H. B. Li, A. Pirrotta, K. Börjesson, G. C. Solomon, J. Hihath, K. Moth-Poulsen, *J. Phys. Chem. C* **2017**, *121*, 7094–7100.

[19] K. Jorner, A. Dreos, R. Emanuelsson, O. El Bakouri, I. F. Galván, K. Börjesson, F. Feixas, R. Lindh, B. Zietz, K. Moth-Poulsen, et al., *J. Mater. Chem. A* **2017**, *5*, 12369–12378.

[20] M. J. Kuisma, A. M. Lundin, K. Moth-Poulsen, P. Hyldgaard, P. Erhart, *J. Phys. Chem. C* **2016**, *120*, 3635–3645.

[21] M. Mansø, A. U. Petersen, Z. Wang, P. Erhart, M. B. Nielsen, K. Moth-Poulsen, *Nat. Commun.* **2018**, *9*.

[22] A. Dreos, Z. Wang, J. Udmark, A. Ström, P. Erhart, K. Börjesson, M. B. Nielsen, K. Moth-Poulsen, *Adv. Energy Mater.* **2018**, *8*.

[23] O. Brummel, D. Besold, T. Döpper, Y. Wu, S. Bochmann, F. Lazzari, F. Waidhas, U. Bauer, P. Bachmann, C. Papp, et al., *ChemSusChem* **2016**, *9*, 1424–1432.

[24] M. Alemani, M. V. Peters, S. Hecht, K. H. Rieder, F. Moresco, L. Grill, *J. Am. Chem. Soc.* **2006**, *128*, 14446–14447.

[25] D. I. Gittins, D. Bethell, D. J. Schiffrin, R. J. Nichols, *Nature* **2000**, *408*, 67–69.

[26] C. P. Collier, G. Mattersteig, E. W. Wong, Y. Luo, K. Beverly, J. Sampaio, F. M. Raymo, J. F. Stoddart, J. R. Heath, *Science (80-.).* **2000**, *289*, 1172–1175.

[27] M. Tsutsui, M. Taniguchi, K. Yokota, T. Kawai, *Appl. Phys. Lett.* **2010**, *96*.

[28] D. R. Ward, D. A. Corley, J. M. Tour, D. Natelson, *Nat. Nanotechnol.* **2011**, *6*, 33–38.

[29] Y. Zhang, H. Fujisaki, J. E. Straub, *J. Phys. Chem. B* **2007**, *111*, 3243–3250.

[30] S. A. Kovalenko, R. Schanz, H. Hennig, N. P. Ernsting, *J. Chem. Phys.* **2001**, *115*, 3256–3273.

[31] C. T. Middleton, B. Cohen, B. Kohler, *J. Phys. Chem. A* **2007**, *111*, 10460–10467.

[32] O. Braem, T. J. Penfold, A. Cannizzo, M. Chergui, *Phys. Chem. Chem. Phys.* **2012**, *14*, 3513–3519.

[33] Y. Selzer, L. Cai, M. A. Cabassi, Y. Yao, J. M. Tour, T. S. Mayer, D. L. Allara, *Nano Lett.* **2005**, *5*, 61–65.

[34] A. L. Tchougréeff, A. M. Tokmachev, R. Dronskowski, *Int. J. Quantum Chem.* **2013**, *113*, 1833–1846.

[35] G. F. Koser, J. N. Faircloth, *J. Org. Chem.* **1976**, *41*, 583–585.

[36] R. W. Hoffmann, W. Barth, *J. Chem. Soc. Chem. Commun.* **1983**, 345–346.

[37] P. G. Gassman, J. W. Hershberger, *J. Org. Chem.* **1987**, *52*, 1337–1339.

[38] F. Chen, J. He, C. Nuckolls, T. Roberts, J. E. Klare, S. Lindsay, *Nano Lett.* **2005**, *5*, 503–506.

[39] A. Migliore, P. Schiff, A. Nitzan, *Phys. Chem. Chem. Phys.* **2012**, *14*, 13746–13753.

[40] B. M. Briechle, Y. Kim, P. Ehrenreich, A. Erbe, D. Sysoiev, T. Huhn, U. Groth, E. Scheer, *Beilstein J. Nanotechnol.* **2012**, *3*, 798–808.

[41] R. Frisenda, M. L. Perrin, H. Valkenier, J. C. Hummelen, H. S. J. Van der Zant, *Phys. Status Solidi Basic Res.* **2013**, *250*, 2431–2436.

[42] A. C. Aragonès, N. L. Haworth, N. Darwish, S. Ciampi, N. J. Bloomfield, G. G. Wallace, I. Diez-Perez, M. L. Coote, *Nature* **2016**, *531*, 88–91.

[43] Z. Ioffe, T. Shamai, A. Ophir, G. Noy, I. Yutsis, K. Kfir, O. Cheshnovsky, Y. Selzer, *Nat. Nanotechnol.* **2008**, *3*, 727–732.

Table of Contents

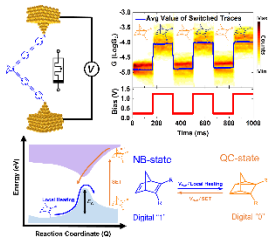

This work demonstrates an electrically controllable single-molecule level reaction. The reversible reaction can be electrically controlled to perform switching and memory functions, where the conductance values of two molecular isomers are encoded as “0” and “1”. Multiple cycles of switching behavior is observed when applied a voltage signal and the absence of stochastic switching suggests the application as a memory device.